Title
Control of pain initiation by endogenous cannabinoids

Journal
Nature, 394(6690)

ISSN
0028-0836

Authors
Calignano, Antonio
Rana, Giovanna La
Giuffrida, Andrea
et al.

Publication Date
1998-07-01

DOI
10.1038/28393

of this comparison is easier to establish, especially for Braille readers about whom there is little information on pseudoword processing.

Auditory stimuli had the same characteristics as the visual/tactile stimuli except that the non-words were reversed words. During half of the word-presentation conditions, we presented abstract words (low imageability 250–400 (according to the Medical Research Council psycholinguistic database)) and concrete words (high imageability 550–700). The task in all conditions was a feature-detection task involving incidental word processing as described previously[3]. Targets were ascenders in the visual conditions (for example in the letters l, d and t), one or more raised dot number 6 (the right lower dot) in the Braille words, and a short tone in the auditory conditions. The use of implicit processing allowed us to match attentional set between conditions and to monitor performance. Words and non-words were matched for the number of characters (5.6 ± 1.3), syllables (1.7 ± 0.5) and occurrences of targets (49%). Responses were made by pressing a button with the thumb of the right hand. The instructions were: "Read/listen to the word and if you find/hear a target, press the button". Target detection exceeded 85% in all groups. The mean reaction time for visual/tactile presentation was 552 ± 116 ms for the sighted group, 1,605 ± 281 ms for the congenitally blind group and 1,809 ± 364 ms for the late-blind group.

Received 6 April; accepted 27 May 1998.

1. Rapcsak, S. Z., Gonzalez Rothi, L. J. & Heilman, K. M. Phonological alexia with optic and tactile anomia: a neuropsychological and anatomical study. *Brain Lang.* **31,** 109–121 (1987).
2. Damasio, A. R. & Damasio, H. The anatomic basis of pure alexia. *Neurology* **33,** 1573–1583 (1983).
3. Price, C. J., Wise, R. J. S. & Frackowiak, R. S. J. Demonstrating the implicit processing of visually presented words and pseudowords. *Cerebral Cortex* **6,** 62–70 (1996).
4. Petersen, S. E., Fox, P. T., Snyder, A. Z. & Raichle, M. E. Activation of extrastriate and frontal cortical areas by words and word-like stimuli. *Science* **249,** 1041–1044 (1990).
5. Price, C. J. & Friston, K. J. Cognitive conjunction: a new approach to brain activation experiments. *Neuroimage* **5,** 261–270 (1997).
6. Puce, A., Allison, T., Asgari, M., Gore, J. C. & McCarthy, G. Differential sensitivity of human visual cortex to faces, letterstrings, and textures: a functional magnetic resonance imaging study. *J. Neurosci.* **16,** 5205–5215 (1996).
7. Bookheimer, S. Y., Zeffiro, T. A., Blaxton, T., Gaillard, W. & Theodore, W. Regional cerebral blood flow during object naming and word reading. *Hum. Brain Mapp.* **3,** 93–106 (1995).
8. Brunswick, N., McCroy, E., Price, C., Frith, C. D. & Frith, U. Explicit and implicit processing of words and pseudowords by adult developmental dyslexics: a search for Wernicke's Wortschatz? *Brain* (submitted).
9. Rumsey, J. M. *et al.* A positron emission tomographic study of impaired word recognition and phonological processing in dyslexic men. *Arch. Neurol.* **54,** 562–573 (1997).
10. Damasio, A. R. & Damasio, H. in *Large Scale Neuronal Theories of the Brain* (eds Koch, C. & Davis, J. L.) 61–74 (MIT Press, Cambridge, MA, 1994).
11. Ungerleider, L. G. & Haxby, J. V. 'What' and 'where' in the human brain. *Curr. Opin. Neurobiol.* **4,** 157–165 (1994).
12. Haxby, J. V. *et al.* Dissociation of object and spatial visual processing pathways in human extrastriate cortex. *Proc. Natl Acad. Sci. USA* **88,** 1621–1625 (1991).
13. Nobre, A. C., Allison, T. & McCarthy, G. Word recognition in the human inferior temporal lobe. *Nature* **372,** 260–263 (1994).
14. Luders, H. *et al.* Basal temporal language area demonstrated by electrical stimulation. *Neurology* **36,** 505–510 (1986).
15. Burnstine, T. H. *et al.* Characterization of the basal temporal language area in patients with left temporal lobe epilepsy. *Neurology* **40,** 966–970 (1990).
16. Farah, M. J. *Visual Agnosia* (MIT Press, Cambridge, MA, 1990).
17. Allison, T., McCarthy, G., Nobre, A., Puce, A. & Belger, A. Human extrastriate visual cortex and the perception of faces, words, numbers, and colors. *Cerebral Cortex* **4,** 544–554 (1994).
18. Kanwisher, N., McDermott, J. & Chun, M. M. The fusiform face area: a module in human extrastriate cortex specialized for face perception. *J. Neurosci.* **17,** 4302–4311 (1997).
19. Sadato, N. *et al.* Activation of the primary visual cortex by Braille reading in blind subjects. *Nature* **380,** 526–528 (1996).
20. Büchel, C., Price, C. J., Frackowiak, R. S. J. & Friston, K. J. Different activation patterns in the occipital cortex of late and congenitally blind subjects. *Brain* **121,** 409–419 (1998).
21. Fiez, J. A. *et al.* PET studies of auditory and phonological processing—effects of stimulus characteristics and task demands. *J. Cog. Neurosc.* **7,** 357–375 (1995).
22. Martin, A., Haxby, J. V., Lalonde, F. M., Wiggs, C. L. & Ungerleider, L. G. Discrete cortical regions associated with knowledge of color and knowledge of action. *Science* **270,** 102–105 (1995).
23. Desposito, M. *et al.* A functional MRI study of mental image generation. *Neuropsychol.* **35,** 725–730 (1997).
24. Suzuki, W. A., Zola-Morgan, S., Squire, L. R. & Amaral, D. G. Lesions of the perirhinal and parahippocampal cortices in the monkey produce long-lasting memory impairment in the visual and tactile modalities. *J. Neurosci.* **13,** 2430–2451 (1993).
25. De Renzi, E., Zambolin, A. & Crisi, G. The pattern of neuropsychological impairment associated with left posterior cerebral-artery infarcts. *Brain* **110,** 1099–1116 (1987).
26. Friedman, R. F., Ween, J. E. & Albert, M. L. in *Clinical Neuropsychology* (eds Heilman, K. M. & Valenstin, E.) 37–62 (Oxford Univ. Press, Oxford, 1993).
27. Foundas, A. L., Daniels, S. K. & Vasterling, J. J. Anomia: case studies with lesion localization. *Neurocase* **4,** 35–43 (1998).
28. Friston, K. J. *et al.* Statistical parametric maps in functional imaging: a general linear approach. *Hum. Brain Mapp.* **2,** 189–210 (1995).

Acknowledgements. The authors are supported by the Wellcome Trust. We thank A. Brennan, A. Carrol, G. Lewington, J. Galliers and S. Grootoonk for their help with data collection, R. Frackowiak, J. Coull and A. Kleinschmidt for an internal review of this manuscript, and M. Rötger for discussions. We are indebted to our subjects, especially the blind subjects and the Royal National Institute for the Blind in the UK.

Correspondence and requests for materials should be addressed to C.B. (e-mail: c.buechel@fil.ion.ucl.ac.uk).

Control of pain initiation by endogenous cannabinoids

Antonio Calignano, Giovanna La Rana, Andrea Giuffrida* & Daniele Piomelli*

Dipartimento di Farmacologia Sperimentale, Università di Napoli, 49 via D. Montesano, Napoli 80131, Italy
** The Neurosciences Institute, 10640 J. J. Hopkins Drive, San Diego, California 92121, USA*

The potent analgesic effects of cannabis-like drugs[1–4] and the presence of CB1-type cannabinoid receptors in pain-processing areas of the brain and spinal cord[5,6] indicate that endogenous cannabinoids such as anandamide[7] may contribute to the control of pain transmission within the central nervous system (CNS)[8]. Here we show that anandamide attenuates the pain behaviour produced by chemical damage to cutaneous tissue by interacting with CB1-like cannabinoid receptors located outside the CNS. Palmitylethanolamide (PEA), which is released together with anandamide from a common phospholipid precursor[9], exerts a similar effect by activating peripheral CB2-like receptors. When administered together, the two compounds act synergistically, reducing pain responses 100-fold more potently than does each compound alone. Gas-chromatography/mass-spectrometry measurements indicate that the levels of anandamide and PEA in the skin are enough to cause a tonic activation of local cannabinoid receptors. In agreement with this possibility, the CB1 antagonist SR141716A and the CB2 antagonist SR144528 prolong and enhance the pain behaviour produced by tissue damage. These results indicate that peripheral CB1-like and CB2-like receptors participate in the intrinsic control of pain initiation and that locally generated anandamide and PEA may mediate this effect.

Although pain perception is thought to be controlled mainly by neurotransmitter systems that operate within the CNS[10], antinociceptive (pain-relieving or -preventing) mechanisms also occur in peripheral tissues. For example, endogenous opioid peptides released from activated immune cells during inflammation inhibit pain transmission by interacting with opioid receptors on peripheral sensory nerve endings[11]. To determine whether endogenous cannabinoids have an analogous function to that of opioids, we used the formalin test, a behavioural model of injury-induced acute and tonic pain[12]. Injection of dilute formalin into the hind paws of freely moving rodents evokes a pain behaviour consisting of two temporally distinct phases of licking and flexing of the injected limb[12]. An early phase involving acute activation of pain-sensing C fibres[13] begins immediately after formalin administration, reaches a peak within 5 min, and then rapidly declines. After an interval of 10–15 min, a second phase of sustained pain behaviour appears, in which sensory fibre activity is accompanied by inflammation[14] and central sensitization[15].

Table 1 Effects of anandamide and PEA on the behavioural response to acute thermal stimuli

	Hot-plate latencies (s)			
Time (min)	Vehicle	AEA	PEA	AEA/PEA
5	24 ± 2	24 ± 4	22 ± 3	25 ± 2
10	24 ± 2	23 ± 3	23 ± 3	26 ± 4
15	22 ± 3	29 ± 3	21 ± 2	30 ± 3
20	25 ± 2	35 ± 2*	25 ± 4	37 ± 3*
30	25 ± 3	40 ± 3*	26 ± 5	39 ± 2*
40	25 ± 3	30 ± 3	22 ± 4	35 ± 5
60	26 ± 2	28 ± 3	24 ± 2	26 ± 3

Time delays to the response were measured at certain times (in min) after intracerebroventricular administration of vehicle (10% DMSO in saline, 5 μl), anandamide (AEA, 10 μg), PEA (10 μg) or anandamide plus PEA (10 μg each). Asterisk indicates $P < 0.01$ ($n = 6$).

In mice, the early phase of pain behaviour was blocked when anandamide was injected into the paw together with formalin, whereas both phases were blocked by the synthetic cannabinoid agonists WIN-55212-2 and HU-210 (Fig. 1a; data not shown). These analgesic effects were prevented by systemic administration of the CB1 antagonist SR141716A (Fig. 1a), but not of the CB2 antagonist SR144528 (Fig. 1a)[16] or of the opioid antagonist naloxone (0.2 mg per kg, intravenous; data not shown). The lack of effect of anandamide on late-phase pain behaviour may be explained by the short lifespan of this compound, which undergoes rapid biological inactivation in tissues[17,18]. In support of this suggestion, the inactivation-resistant analogue methanandamide inhibited pain behaviour during the entire test (Fig. 1a).

Local anandamide injections were not accompanied by central signs of cannabimimetic activity, indicating a peripheral site of action. To test this possibility, we measured the antinociceptive potency of anandamide following local (intraplantar, i.pl.), intravenous (i.v.) or intraperitoneal (i.p.) administrations. Anandamide was 100 times more potent in preventing formalin-evoked pain behaviour when injected locally rather than intravenously, with half-maximal inhibitory doses (ID_{50} values) of 0.1 mg per kg and 10 mg per kg, respectively (Fig. 1b). Anandamide had no significant effect when injected intraperitoneally (Fig. 1b). As a further test, we determined the biodistribution of ^{3}H-labelled anandamide 10 min after i.pl. injection in rats. In three experiments, we found that 94% of recovered ^{3}H-labelled anandamide remained associated with the injected paw (6648 ± 820 d.p.m. per g, mean ± s.e.m.), whereas little or no radioactivity above background was detected in forebrain, cerebellum and spinal cord (79 ± 19; 165 ± 67; and 90 ± 48 d.p.m. per g, respectively). These results indicate that anandamide inhibits nociception after formalin injection by activating CB1-like receptors, which may be located on peripheral endings of sensory neurons involved in pain transmission[5,6].

Anandamide is the ethanolamide of arachidonic acid and is thought to be produced by phosphodiesterase-mediated cleavage of *N*-arachidonyl phosphatidylethanolamine[9,19]. Enzymatic cleavage of other *N*-acyl phosphatidylethanolamines may give rise to additional fatty acylethanolamides, the physiological roles of which are still poorly understood[20]. PEA, an acylethanolamide found in neural and non-neural tissues, inhibits mast-cell activation and reduces inflammatory responses by a mechanism that may involve binding to CB2-like receptors[23]. The molecular identity of these receptors is unknown, although they are likely to be distinct from the CB2 receptors whose encoding genes have been cloned, as PEA shows little or no affinity for these receptors[24]. We found that PEA, but not two closely related analogues, inhibited both early and late phases of formalin-evoked pain behaviour after i.pl. injection in mice (Fig. 2a). This effect may not be explained by the anti-inflammatory properties of PEA; 30 min after injection, the analgesic effects of PEA were not accompanied by a reduction in inflammatory oedema (volumes injected into the paw in ml were: control, 0.18 ± 0.003; formalin, 0.37 ± 0.006; formalin plus 50 μg PEA, 0.35 ± 0.006), which became apparent only 1 h after formalin administration[22].

The analgesia produced by PEA was reversed by administration of the CB2 antagonist SR144528 (Fig. 2a), whereas the CB1 antagonist SR141716A and the opioid antagonist naloxone were ineffective (Fig. 2a; data not shown). In addition, PEA was more potent when administered locally (i.pl.) than systemically (i.v. or i.p.) (Fig. 2b). Together, these results indicate that PEA exerts antinociceptive

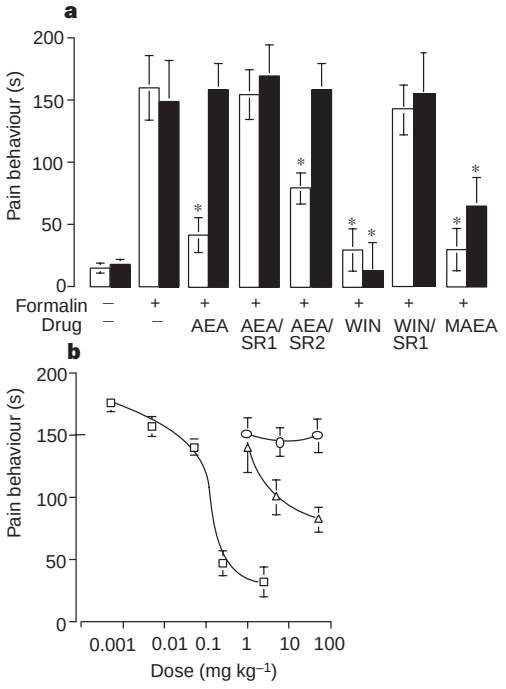

Figure 1 Anandamide inhibits formalin-evoked nociception by activating peripheral CB1-like cannabinoid receptors. **a**, Effects of anandamide (AEA, 50 μg i.pl.), WIN-55212-2 (WIN, 500 μg i.pl.) and methanandamide (MAEA, 50 μg i.pl.), in the absence or presence of the CB1 antagonist SR141716A (SR1, 0.1 mg per kg i.v.) or the CB2 antagonist SR144528 (SR2, 0.1 mg per kg i.v.). Open columns represent the early phase and filled columns the late phase of formalin-evoked nociception. Asterisk indicates $P < 0.01$ (n = 12–18 for each condition). **b**, Dose-dependent antinociceptive effects of anandamide following i.pl. (squares), i.v. (triangles) or i.p. (circles) administration.

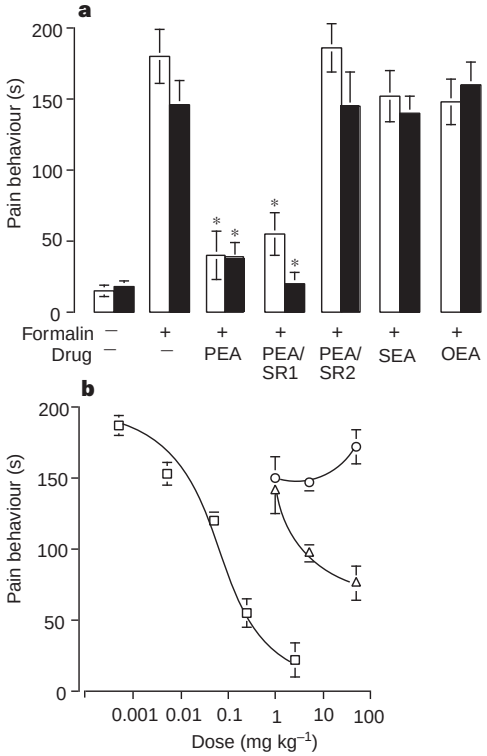

Figure 2 PEA inhibits formalin-evoked nociception by activating peripheral CB2-like cannabinoid receptors. **a**, Effects of PEA (50 μg i.pl.), stearylethanolamide (SEA, 50 μg i.pl.) and oleylethanolamide (OEA, 50 μg i.pl.), in the absence or presence of the CB1 antagonist SR141716A (SR1, 0.1 mg per kg i.v.) or the CB2 antagonist SR144528 (SR2, 0.1 mg per kg i.v.). Open columns represent the early phase and filled columns the late phase of formalin-evoked nociception. Asterisk indicates $P < 0.01$ (n = 12–18). **b**, Dose-dependent antinociceptive effects of PEA following i.pl. (squares), i.v. (triangles) or i.p. (circles) administration.

effects that are mediated by peripheral CB2-like receptors. The cellular localization of such receptors and their possible structural relationship with the CB2 receptor whose gene has been cloned, which is primarily expressed in immune cells[25], are unknown.

The fact that anandamide and PEA activate pharmacologically distinct receptors and that these two substances can be produced simultaneously in tissues[9] prompted us to examine their possible interactions *in vivo*. When injected together in equal amounts, anandamide and PEA inhibited the early phase of formalin-evoked pain behaviour with a potency that was approximately 100-fold greater than each of the compounds separately (Fig. 3a). A similar synergistic potentiation occurred in the late phase, on which anandamide had no effect when given alone (Figs 1a and 3b). Earlier administration of either CB1 or CB2 antagonists entirely blocked the response (Fig. 3c). This interaction did not appear to involve pain-processing structures within the brain: injection of PEA in the cerebral ventricles did not affect the behavioural responses to acute thermal stimuli, assessed in the hot-plate test, and did not enhance the inhibitory activity of anandamide administered by the same route (Table 1). These results indicate that the parallel activation of peripheral CB1- and CB2-like receptors by anandamide and PEA results in a synergistic inhibition of peripheral pain initiation.

To test this idea further, we determined the intrinsic effects of CB1 and CB2 antagonists on formalin-evoked pain behaviour (Fig. 4). Blockade of CB1 receptors with SR141716A produced significant hyperalgesia (Fig. 4a)[8]. This effect was particularly pronounced after local injection of the drug, which resulted in a 10-min prolongation of the early nociceptive phase and in a two- to threefold increase in pain behaviour during the entire testing period (Fig. 4b). In contrast, systemic administration of the CB2 antagonist SR144528 caused a selective enhancement of early-phase, but not of late-phase, responses (Fig. 4a). The selectivity of this effect may not result from a rapid elimination of SR144528 after early phase, as the drug reversed PEA-induced antinociception during both early- and late-phase pain behaviour (Fig. 2). SR144528 could not be administered locally because of its limited solubility in the injection vehicle.

Although the hyperalgesic effects of CB1 and CB2 antagonists may be accounted for by their inverse agonist properties[16,26], two lines of evidence suggest that these drugs acted by removing an endogenous cannabinoid tone. First, gas-chromatography/mass-spectrometry analyses showed that anandamide and PEA are present in

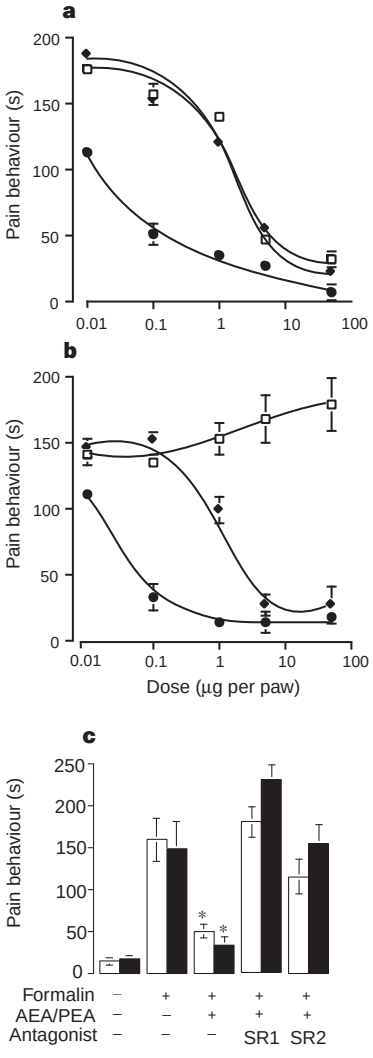

Figure 3 Anandamide and PEA synergistically inhibit formalin-evoked nociception. **a**, Early phase. **b**, Late phase (open squares, anandamide; filled diamonds, PEA; filled circles, anandamide plus PEA). Equal amounts of anandamide and PEA were administered by i.pl. injection at the doses indicated on the abscissa. **c**, The CB1 antagonist SR141716A (SR1) and the CB2 antagonist SR144528 (SR2) prevent the effects of anandamide plus PEA (0.1 μg each of anandamide and PEA). Open columns represent the early phase and closed columns the late phase of formalin-evoked nociception. Antagonists were administered by i.v. injection at the dose of 0.1 mg per kg. Asterisk denotes $P < 0.01$ ($n = 12$).

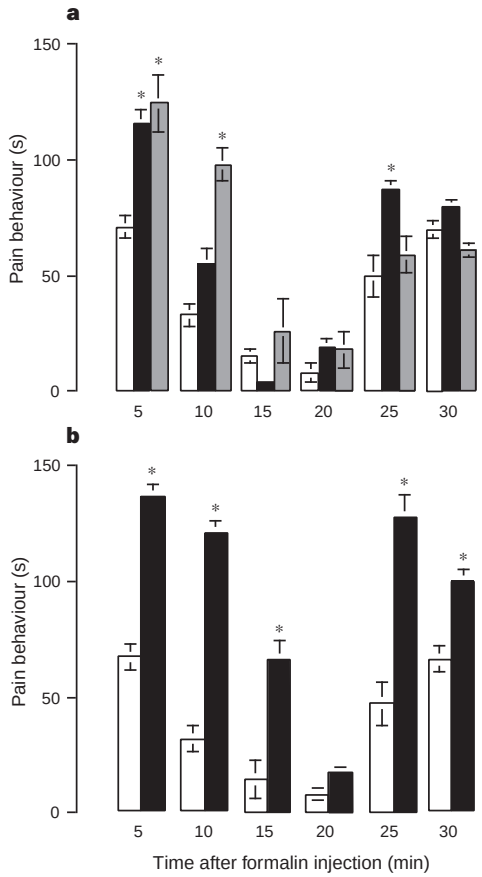

Figure 4 Intrinsic hyperalgesic effects of cannabinoid antagonists on the time course of formalin-evoked nociception. **a**, Effects of systemic administration of the CB1 antagonist SR141716A (filled bars) and the CB2 antagonist SR144528 (grey shaded bars). The drugs were administered by i.v. injection at 0.1 mg per kg. The responses to formalin alone are shown by open bars. **b**, Effects of local administration of SR141716A (filled bars). 10 μg of SR141716A were administered with formalin by i.pl. injection. SR144528 was not soluble in 10% DMSO, and could not be injected locally. Asterisk denotes $P < 0.01$ ($n = 6$).

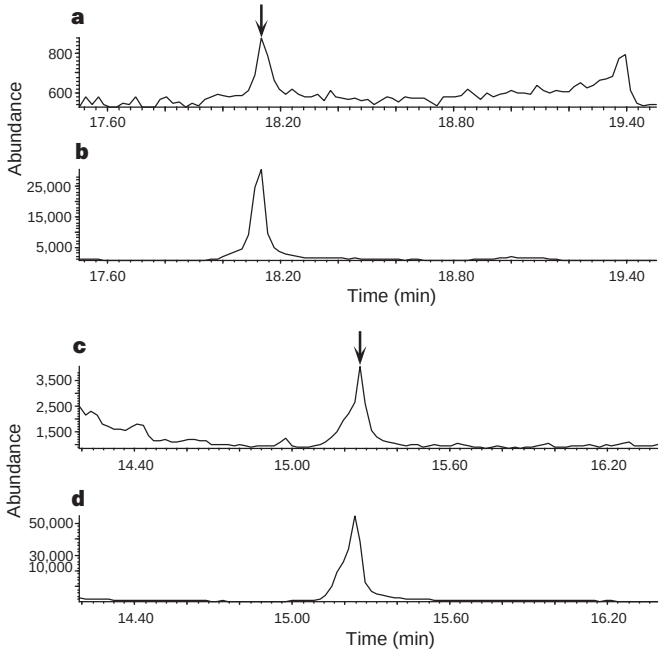

Figure 5 Identification by gas chromatography/mass spectrometry of anandamide and PEA in rat paw skin. **a**, **b**, Representative tracings for selected fragments characteristic of endogenous anandamide (**a**, mass-to-charge ratio $m/z = 404$, $[M-15]^+$, a fragment produced by loss of one methyl group) and synthetic [$^2H_4$]anandamide (**b**, $m/z = 408$) which was added to the samples as an internal standard. **c**, **d**, Representative tracings for fragments characteristic of endogenous PEA (**c**, $m/z = 356$, $[M-15]^+$) and standard [$^2H_4$]PEA (**d**, $m/z = 360$). The results are from one experiment and are typical of eight experiments.

rat paw skin (Fig. 5). By comparison with internal deuterated standards, we measured 49 ± 9 pmol of anandamide and 692 ± 119 pmol of PEA per g of tissue ($n = 8$). These amounts are five- to tenfold higher than those measured by the same method in rat brain and plasma[27,28], and are probably sufficient to activate cannabinoid receptors[7,23]. Second, the CB2 antagonist SR144528 enhanced nociception selectively during the early phase of the formalin response (Fig. 4a), a result inconsistent with an inverse agonist effect. Thus, a parsimonious interpretation of our findings is that endogenous PEA acting at CB2-like receptors may participate in attenuating the early stages of nociception, whereas endogenous anandamide acting at CB1-like receptors may have a more sustained modulatory effect on both acute and tonic pain.

Our results show that the tonic activation of local CB1-like and CB2-like receptors may regulate pain initiation in cutaneous tissue. These findings support the possibility that endogenous cannabinoids, in addition to their spinal and supraspinal sites of action[8], may participate in buffering emerging pain signals at sites of tissue injury. The results also indicate that selective agonists for the CB2-like receptor activated by PEA, or peripherally administered CB1-like/CB2-like agonists, may reduce pain without the dysphoric side effects and perceived abuse potential typical of centrally acting cannabimimetic or opiate drugs.

Note added in proof: After submission of this paper, Jaggar *et al.*[29] have observed an analgesic effect of systemically administered PEA in formalin-induced pain. □

Methods

Drugs. Anandamide, PEA, stearylethanolamide and oleylethanolamide were synthesized following standard procedures[7]; SR144528 {*N*-[(1S)-endo-1, 3, 3-trimethyl bicyclo [2.2.1] heptan-2-yl]-5-(4-chloro-3-methylphenyl)-1-(4-methylbenzyl)-pyrazole-3-carboxamide} was a gift from Sanofi; SR141716A {[*N*-(piperidin-1-yl)-5-(4-chlorophenyl)-1-(2,4-dichlorophenyl)-4-methyl-1-H-pyrazole-3-carboxamide·HCl]} was provided by RBI as part of the Chemical Synthesis Program of the NIMH; all other drugs were from Tocris. The drugs were dissolved in dimethylsulphoxide (DMSO) and administered in physiological saline containing 10% DMSO; volumes injected were 0.2 ml i.v. and i.p. and 0.01 ml i.pl.

Nociceptive tests. Saline (10 μl) containing 5% formalin and 10% DMSO was injected subcutaneously into the hind paws of male Swiss mice (20–25 g in weight; Nossan). The duration of paw licking was monitored by an observer blind to the experimental treatment for periods of 0–15 min (early phase) and 15–30 min (late phase) after formalin administration. Initial tests determined that the presence of 10% DMSO in the injection vehicle did not significantly affect formalin responses (data not shown). For the experiment in Fig. 4, pain behaviour was monitored for 5-min periods during the 30 min following formalin injection. Time delays to escape jumping or hind-paw licking were measured on a plate heated to 55.5 °C, according to standard procedures[18].

Inflammation. Inflammatory oedemas were produced in the hind paws of Swiss mice by injection of saline (10 μl) containing 5% formalin and 10% DMSO, and were measured with a plethysmometer[22] (Ugo Basile).

Gas chromatography/mass spectrometry (GC/MS). Hairless paw skin tissue was excised from Wistar rats anaesthetized with nembutal, and immediately immersed in cold methanol to prevent alterations in tissue lipids. After homogenization and chloroform/methanol extraction, high-performance liquid chromatography and quantitative analysis of the trimethyl silyl derivatives of anandamide and PEA by isotope dilution GC/MS were carried out as described[28].

Data analysis. Results are expressed as means ± s.e.m. The significance of differences between groups was evaluated using analysis of variance with a subsequent Dunnett's test.

Received 19 January; accepted 20 April 1998.

1. Martin, B. R., Balster, R. L., Razdan, R. K., Harris, L. S. & Dewey, W. L. Behavioral comparisons of the stereoisomers of tetrahydrocannabinols. *Life Sci.* **20,** 565–574 (1981).
2. Martin, W. J., Lai, N. K., Patrick, S. L., Tsou, K. & Walker, J. M. Antinociceptive actions of cannabinoids following intraventricular administration in rats. *Brain Res.* **629,** 300–304 (1993).
3. Tsou, K. *et al.* Suppression of noxious stimulus-evoked expression of FOS protein-like immunoreactivity in rat spinal cord by a selective cannabinoid agonist. *Neuroscience* **70,** 791–798 (1996).
4. Lichtman, A. H., Cook, S. A. & Martin, B. R. Investigation of brain sites mediating cannabinoid-induced antinociception in rats: evidence supporting periaqueductal gray involvement. *J. Pharmacol. Exp. Ther.* **276,** 585–593 (1996).
5. Herkenham, M. *et al.* Cannabinoid receptor localization in brain. *Proc. Natl Acad. Sci. USA* **87,** 1932–1936 (1990).
6. Tsou, K., Brown, S., Sañudo-Peña, M. C., Mackie, K. & Walker, J. M. Immunohistochemical distribution of cannabinoid CB1 receptors in the rat central nervous system. *Neuroscience* **83,** 393–411 (1998).
7. Devane, W. *et al.* Isolation and structure of a brain constituent that binds to the cannabinoid receptor. *Science* **258,** 1946–1949 (1992).
8. Richardson, J. D., Aanonsen, L. & Hargreaves, K. M. Hypoactivity of the spinal cannabinoid system results in NMDA-dependent hyperalgesia. *J. Neurosci.* **18,** 451–457 (1998).
9. Di Marzo, V. *et al.* Formation and inactivation of endogenous cannabinoid anandamide in central neurons. *Nature* **372,** 686–691 (1994).
10. Fields, H. L. *Pain* (McGraw-Hill, New York, 1987).
11. Stein, C. The control of pain in peripheral tissue by opioids. *New Engl. J. Med.* **332,** 1685–1690 (1995).
12. Dubuisson, D. & Dennis, S. G. The formalin test: a quantitative study of the analgesic effects of morphine, meperidine, and brain stem stimulation in rats and cats. *Pain* **4,** 161–174 (1977).
13. Dickenson, A. H. & Sullivan, A. F. Subcutaneous formalin-induced activity of dorsal horn neurones in the rat: differential response to an intrathecal opiate administered pre or post formalin. *Pain* **30,** 349–360 (1987).
14. Rosland, J. H., Tjølsen, A., Maehle, B. & Hole, K. The formalin test in mice: effect of formalin concentration. *Pain* **42,** 235–242 (1990).
15. Coderre, T. J. & Melzack, R. The contribution of excitatory amino acids to central sensitization and persistent nociception after formalin-induced tissue injury. *J. Neurosci.* **12,** 3665–3670 (1992).
16. Rinaldi-Carmona, M. *et al.* SR 144528, the first potent and selective antagonist of the CB2 cannabinoid receptor. *J. Pharmacol. Exp. Ther.* **284,** 644–650 (1998).
17. Cravatt, B. F. *et al.* Molecular characterization of an enzyme that degrades neuromodulatory fatty-acid amides. *Nature* **384,** 83–87 (1996).
18. Beltramo, M. *et al.* Functional role of high-affinity anandamide transport, as revealed by selective inhibition. *Science* **277,** 1094–1097 (1997).
19. Cadas, H., di Tomaso, E. & Piomelli, D. Occurrence and biosynthesis of endogenous cannabinoid precursor, N-arachidonoyl phosphatidylethanolamine, in rat brain. *J. Neurosci.* **17,** 1226–1242 (1997).
20. Schmid, H. H. O., Schmid, P. C. & Natarajan, V. The N-acylation-phosphodiesterase pathway and cell signalling. *Chem. Phys. Lipids* **80,** 133–142 (1996).
21. Aloe, L., Leon, A. & Levi-Montalcini, R. A proposed autacoid mechanism controlling mastocyte behaviour. *Agents Actions* **39,** C145–C147 (1993).
22. Mazzari, S., Canella, R., Petrelli, L., Marcolongo, G. & Leon, A. N-(2-hydroxyethyl)hexadecanamide is orally active in reducing edema formation and inflammatory hyperalgesia by down-modulating mast cell activation. *Eur. J. Pharmacol.* **300,** 227–236 (1996).
23. Facci, L. *et al.* Mast cells express a peripheral cannabinoid receptor with differential sensitivity to anandamide and palmitoylethanolamide. *Proc. Natl Acad. Sci. USA* **92,** 3376–3380 (1995).
24. Showalter, V. M., Compton, D. R., Martin, B. R. & Abood, M. E. Evaluation of binding in a transfected cell line expressing a peripheral cannabinoid receptor (CB2): identification of cannabinoid receptor subtype selective ligands. *J. Pharmacol. Exp. Ther.* **278,** 989–999 (1996).
25. Munro, S., Thomas, K. L. & Abu-Shaar, M. Molecular characterization of a peripheral receptor for cannabinoids. *Nature* **365,** 61–65 (1993).

26. Landsman, R. S., Burkey, T. H., Consroe, P., Roeske, W. R. & Yamamura, H. I. SR141716A is an inverse agonist at the human cannabinoid CB1 receptor. *Eur. J. Pharmacol.* **334,** R1–R2 (1997).
27. Stella, N., Schweitzer, P. & Piomelli, D. A second endogenous cannabinoid that modulates long-term potentiation. *Nature* **388,** 773–778 (1997).
28. Giuffrida, A. & Piomelli, D. Isotope dilution GC/MS determination of anandamide and other fatty acylethanolamides in rat blood plasma. *FEBS Lett.* **422,** 373–376 (1998).
29. Jaggar, S. I., Hasnie, F. S., Sellatwray, S. & Rice, A. S. C. The antihyperalgesic actions of the cannabinoid anandamide and the putative CB2 receptor agonist palmitoylethanolamide in visceral and somatic inflammatory pain. *Pain* (in the press).

Acknowledgements. We thank P. Cimminiello, F. De Seta and V. Piscicelli for experimental assistance, and M. Beltramo, A. Makriyannis, L. Sorrentino and N. Stella for discussion. Supported by Neurosciences Research Foundation (A.G. and D.P.), which receives major support from Novartis, and by MURST (G.L.R. and A.C.).

Correspondence and requests for materials should be addressed to D.P. (e-mail: piomelli@nsi.edu).

Expression of a potassium current in inner hair cells during development of hearing in mice

Corné J. Kros*†, J. Peter Ruppersberg‡§ & Alfons Rüsch†‡§

* *Department of Physiology, School of Medical Sciences, University of Bristol, University Walk, Bristol BS8 1TD, UK*
† *School of Biological Sciences, University of Sussex, Falmer, Brighton BN1 9QG, UK*
‡ *Department of Physiology, University of Tübingen, Gmelinstraße 5, 72076 Tübingen, Germany*
§ *Division of Sensory Biophysics, ENT Hospital, University of Tübingen, Röntgenweg 11, 72076 Tübingen, Germany*
† *These authors contributed equally to this work.*

Excitable cells use ion channels to tailor their biophysical properties to the functional demands made upon them[1]. During development, these demands may alter considerably, often associated with a change in the cells' complement of ion channels[2–4]. Here we present evidence for such a change in inner hair cells, the primary sensory receptors in the mammalian cochlea. In mice, responses to sound can first be recorded from the auditory nerve and observed behaviourally from 10–12 days after birth; these responses mature rapidly over the next 4 days[5–8]. Before this time, mouse inner hair cells have slow voltage responses and fire spontaneous and evoked action potentials. During development of auditory responsiveness a large, fast potassium conductance is expressed, greatly speeding up the membrane time constant and preventing action potentials. This change in potassium channel expression turns the inner hair cell from a regenerative, spiking pacemaker into a high-frequency signal transducer.

Substantial changes in the ear's anatomy and in gross cochlear potentials occur around the onset and subsequent rapid maturation of auditory function[7,9–11]. Very little is known, by contrast, about how the membrane currents of the inner and outer hair cells (IHCs and OHCs) develop. We have studied, under whole-cell voltage clamp, time- and voltage-dependent conductances of IHCs, the cells responsible for signalling the reception of sound to the brain, as a function of development between postnatal day (P) 0 and 68.

Before P11–P12, the outward membrane currents of IHCs rise slowly and are fairly small (Fig. 1a). By P13, the outward currents of all cells have acquired an additional fast component (Fig. 1b) which becomes larger over the next few days, as shown for a P19 cell in Fig. 1c. The current–voltage curves of Fig. 1d (filled symbols) show the appearance and the increase in magnitude of the fast component of the outward current that occurs between P11 and P19; this fast component is largely responsible for the increase in total current (open symbols).

The outward currents recorded in mouse IHCs from a few days after the onset of hearing closely resemble the membrane currents described before for mature guinea-pig IHCs, which also have a fast and a slow component equated with two different potassium currents, $I_{K,f}$ (probably carried by BK channels[1,12,13]) and $I_{K,s}$ (a delayed rectifier), respectively[14,15]. The fast component of the current in mouse IHCs is reversibly suppressed by tetraethylammonium (TEA; half-blocking concentration (IC_{50}) estimated from the dose–response curve as 0.30 ± 0.03 mM; $n = 5$), to which the slow component is comparatively resistant ($IC_{50} = 31 \pm 8$ mM, $n = 4$; measured between P17 and P20). The fast component is also blocked by charybdotoxin with an IC_{50} of 21 ± 2 nM ($n = 13$) and by the apparently selective BK-channel-blocker iberiotoxin[16] ($IC_{50} < 10$ nM; $n = 3$). Taken together, this evidence identifies the fast component in mouse IHCs with $I_{K,f}$. The slow component of the mouse K^+ currents is like $I_{K,s}$ in cells studied after the onset of hearing, but the slow current observed at earlier times, in neonatal cells, appears different[15]: it inactivates (slowly) and is considerably more sensitive to block by TEA (IC_{50} 4.6 ± 0.9 mM, $n = 6$; P4–P11); we therefore call it $I_{K,neo}$. The development over time of the different currents is shown in Fig. 2. The total current increases sevenfold between P12 and P16 (Fig. 2a), coincident with the onset and rapid maturation of hearing. Figure 2b shows that this increase is not simply due to the increase in cell capacitance (or membrane area), which is less than twofold, and has a different time course. The increase in total current is mostly contributed by the appearance of $I_{K,f}$ (Fig. 2c): there is an increase in the slow current as well, but it is more gradual (Fig. 2d). In the maturing cochlea, develop-

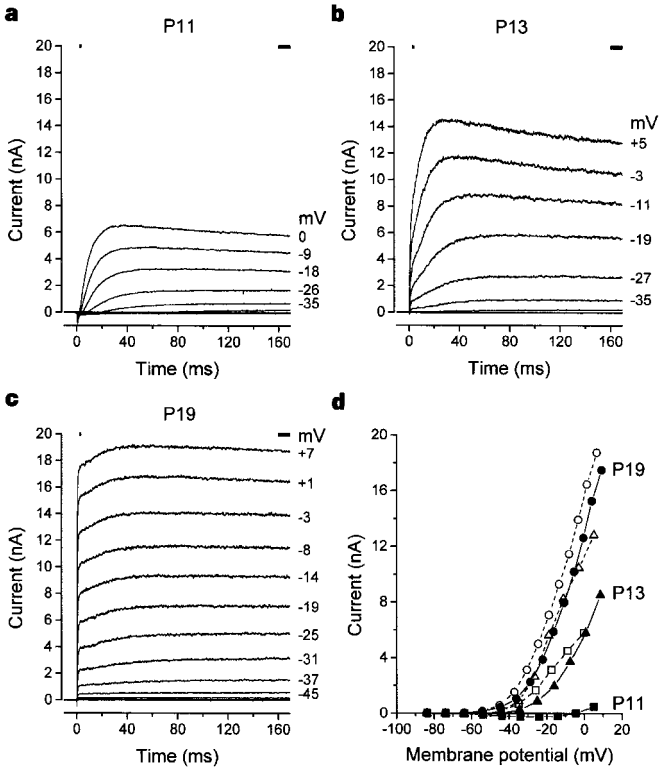

Figure 1 Membrane currents in mouse IHCs of different age. Cells were held at –84 mV, and responses to depolarizations in nominal 10-mV increments were recorded (actual membrane potentials shown by some of the traces). All cells are from the apical coil. Responses are single traces. **a**, At P11, pronounced rapid inward Na^+ currents (over by 2 ms) are followed by outward currents with slow, voltage-dependent kinetics (R_s, 1.0 MΩ, temperature, 24 °C). **b**, At P13, outward currents with extremely fast kinetics precede slow outward currents (0.8 MΩ, 22 °C). **c**, At P19, the adult pattern of currents is established (2.1 MΩ, 24 °C). **d**, Current–voltage curves of the fast component corresponding to $I_{K,f}$ were determined at the time of the short markers in **a**–**c** (filled symbols, solid lines). Total currents were measured at the long markers (open symbols, dashed lines). Squares: P11; triangles: P13; circles: P19.